

Production of Ethyl Cellulose Scaffolds by Supercritical CO₂ Phase Separation

Iolanda De Marco*, Lucia Baldino, Stefano Cardea, Ernesto Reverchon

Department of Industrial Engineering, University of Salerno,
 Via Giovanni Paolo II, 132, 84084, Fisciano (SA), Italy
 idemarco@unisa.it, FAX: 0039-089964057

Ethyl Cellulose scaffolds were prepared using a supercritical fluid phase inversion process in which carbon dioxide acts as the non-solvent.

Ethyl Cellulose is a derivative of cellulose in which some of the hydroxyl groups on the repeating glucose units are converted into ethyl ether groups; it is a biocompatible but non-biodegradable polymer. It is an extensively studied encapsulating material for the controlled release of pharmaceuticals in tissue engineering applications.

Series of experiments were performed at various polymer concentrations, temperatures, pressures, and kind of organic solvent. The structures of the resulting scaffolds were analysed using scanning electron microscopy. We operated with polymer concentrations ranging between 5 and 20 % w/w, using N-methyl pyrrolidone and chloroform as organic solvents and we obtained scaffolds characterized by homogeneous cellular structures with different pore mean size. The mean diameter of the pores ranged from 3 µm to 15 µm, decreasing the polymer concentration from 20 to 5 % w/w. Additional experiments were performed varying the operating pressure from 100 and 200 bar, and varying the operating temperature from 35 to 55 °C. Increasing pressure and/or decreasing temperature, the scaffolds pore size largely decreases; both the effects can be related to carbon dioxide density modification. Ethyl Cellulose scaffolds formation mechanisms were also discussed.

1. Introduction

Tissue engineering (TE) is aiming, primarily, at the regeneration of damaged tissues. This task demands a combination of molecular biology and materials engineering, since in many applications a scaffold is required, that provides a temporary artificial matrix for cell seeding. Scaffolds must meet certain fundamental characteristics such as high porosity, appropriate pore size, biocompatibility, biodegradability and proper degradation rate (Langer and Vacanti, 1993). Furthermore, scaffold fabrication methods should allow for the control of pore size and enhance the maintenance of mechanical properties and material biocompatibility (Langer and Vacanti, 1993; Ma, 2004).

Unfortunately, these methods suffer several limitations; particularly, it is very difficult to obtain simultaneously macro, micro and nanostructural characteristics that are required for the various TE applications. The most used method is the phase separation of a polymeric homogeneous solution (Ho et al., 1995; Schugens et al., 1996a; Schugens et al., 1996b; Hua et al., 2002), in which polymer-poor and polymer-rich liquid phases are generated. The subsequent growth and coalescence of the polymer-poor phase forms pores in the scaffold. In the case of thermally induced phase separation (TIPS), solution temperature is lowered with respect to room temperature to induce the phase separation. It typically leads to the formation of cellular porous structures. When the temperature is low enough, frozen solvent and concentrated polymer phases can be generated due to the solid-liquid demixing mechanism (Kim and Lloyd, 1992). During the subsequent solvent removal, the porous structure needs to be carefully preserved and freeze-drying is usually performed for solvent removal to avoid the collapse of the porous structure (Schugens et al., 1996a; Schugens et al., 1996b). But, this method presents several disadvantages being time consuming and having problems of dense skins formation.

Supercritical fluids assisted processes have been proposed to overcome the limitation of traditional techniques in several fields (Caputo et al., 2010; Cardea et al., 2011; Reverchon et al., 2008; De Marco et

al., 2013) due to their process flexibility and gas-like mass transfer properties. Carbon dioxide is the most commonly used supercritical fluid because it has mild critical parameters, it is environmentally benign, non-toxic, non-flammable, non-corrosive, readily available and inexpensive. Its elimination and the recovery of final products are easy (no residue is left and a dry solid product is obtained, just by controlling the pressure), leading to processes with less energy consumption. Some supercritical carbon dioxide (SC-CO₂) assisted processes have also been proposed for TE applications (Reverchon and Cardea, 2012): supercritical induced phase separation (SC-IPS) (Cardea et al., 2006; Reverchon et al., 2007), supercritical foaming (Mooney et al., 1996; Reverchon and Cardea, 2007), supercritical gel drying combined with particulate leaching (Pisanti et al., 2012; Cardea et al., 2013). The aims of SC-CO₂ assisted techniques in TE is to modulate mass transfer properties, to obtain an efficient solvent elimination, due to the large affinity of SC-CO₂ with almost all the organic solvents, and to work with short processing times, taking advantage of the enhanced mass transfer rates.

Many natural and synthetic polymers were proposed for scaffolding applications, such as poly(glycolic acid) (PGA), poly(lactic acid) (PLA), and their copolymers poly(lactic acid-co-glycolic acid) (PLGA), chitosan and chitin, cellulose-based materials, etc. Cellulose is an abundant and renewable resource found in most parts of the world, which makes it a cheap raw material for various applications (Zeng et al., 2003). However, a limited number of researches have been done until now on the use of cellulose and cellulose derivatives as materials for TE applications. The complications involved in cellulose-based materials are mainly due to the many difficulties ascribed to the material, one being its reluctance to interact with conventional solvents. Therefore, the choice of solvent systems is very important. In particular, Ethyl-cellulose (EC) is a kind of cellulose ether and it is a biocompatible polymer. EC is one of the extensively studied encapsulating materials for the controlled release of pharmaceuticals (Prasertmanakit et al., 2009).

In this work, for the first time, EC scaffolds were obtained by SC-CO₂ phase separation. We verified the feasibility of the process and analyzed the effect of the process parameters (polymer concentration, pressure, temperature, processing time, etc) on the scaffolds morphology, properly characterizing the scaffolds generated.

2. Experimental section

2.1 Materials

Ethyl cellulose (EC, molecular weight 2.5×10^5), n-methyl-2-pyrrolidone (NMP) (purity 99.8 %), and chloroform (purity 99.5 %) were bought from Sigma-Aldrich; carbon dioxide (CO₂) (purity 99 %) was purchased from S.O.N. (Società Ossigeno Napoli, Italy). All materials were processed as received.

2.2 Scaffold preparation

Scaffolds were prepared in a laboratory apparatus equipped with a 316 stainless steel high-pressure vessel with an internal volume of 80 mL, in which SC-CO₂ contacts the polymer solution in a single pass. EC was dissolved in the solvent and the solution obtained was placed in a formation cell (steel caps with a diameter of 2.5 cm and heights of 300 μ m) spreading it with a glass stick to control the thickness of the film. The cell was rapidly put inside the preparation vessel to avoid the evaporation of the solvent. The vessel was, then, closed and filled from the bottom with SC-CO₂, up to the desired pressure using a high-pressure pump (Milton Roy–Milroyal B, France). We operated in batch mode for 45 min; after this period of time, a micrometric valve was opened and the operation was performed in continuous mode; i.e., with a constant CO₂ flow rate at 1.5 kg/h. Pressure and temperature were held constant and the phase-separated structure was dried for 45 min. Then, the vessel was slowly depressurized for 30 min.

2.3 Scanning electron microscopy (SEM).

EC scaffolds were examined by cryofracturing them with a microtome (Bio-optica S.p.A, Italy, Mod. Microm HM 550 OMVP), sputter coating the samples with gold, and viewing them by scanning electron microscope (SEM) (mod. LEO 420, Assing, Italy) to determine pore size and scaffold structure. Sigma Scan Pro 5.0 software (Jandel scientific, San Rafael, CANADA) and Origin 7 software (Microcal, Northampton, USA) were used to determine the average diameter of the pores and to calculate pore size distributions. We measured approximately 350 pores for each scaffold.

2.4 Solvent Residue Analysis

NMP and Chloroform residues were measured by a headspace (HS) sampler (model 7694E, Hewlett Packard, USA) coupled to a gas chromatograph (GC) interfaced with a flame ionization detector (GC-FID, model 6890 GC-SYSTEM, Hewlett Packard, USA).

2.5 Scaffold porosity

The porosity (ϵ) represents the “void space” of the scaffold and was calculated from the density of the scaffold and the density of untreated EC. The scaffold density was determined by measuring its volume and weight. The scaffold volume was obtained using the Archimede’s principle. The scaffolds were waterproofed and subsequently immersed in pure water. Calculating the weight of the displaced water, we evaluated the volume of the sample.

3. Results and discussion

In the first part of the work, we focused our attention on the feasibility of SC-CO₂ phase separation process to generate EC scaffolds. We tested EC at a concentration in NMP of 10 w/w, at a pressure of 150 bar, and at a temperature of 45 °C.

EC/NMP solutions were prepared and processed by SC-CO₂, as reported in the scaffold preparation paragraph. We observed that homogenous cellular structures were obtained; moreover, porosity analyses were performed and values of about 80 % were found. Solvent residue analyses were also performed and values of NMP lower than 5 ppm were found; i.e., as expected, SC-CO₂ phase separation allowed to completely remove the organic solvent of the starting solutions.

Subsequently, we studied the effect of operating parameters on the scaffold morphology and pores size; we performed experiments at different temperatures and pressures, and with polymer concentrations ranging between 5 and 20 % w/w. We verified that, increasing the polymer concentration, the mean pores size decreases. An example is reported in Figure 1, where SEM images taken at the same enlargement of EC scaffolds obtained at 200 bar and 35 °C are reported; it is evident that the EC scaffold obtained starting from a more concentrated solution (20 % w/w – Figure 1a) presents smaller pores than EC scaffold obtained from a more diluted solution (5 % w/w – Figure 1b).

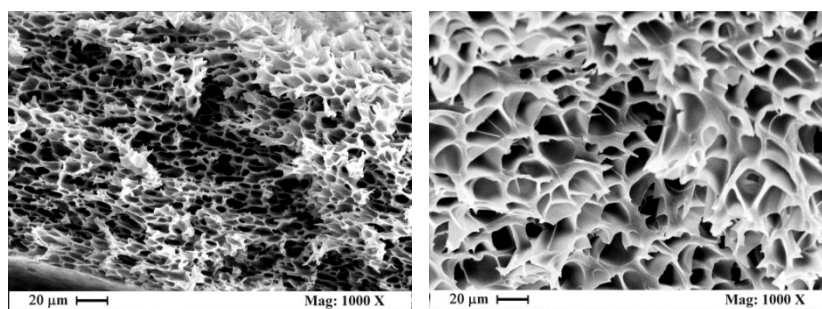


Figure 1: EC scaffolds obtained at 200 bar and 35 °C, starting from 20 % w/w (1a - left) and 5% w/w (1b - right).

This result is in accordance with the theory of the traditional phase separation; indeed, increasing the polymer concentration, the polymer-rich phase increases during the phase separation. As a consequence, smaller pores are generated. This result is quantitatively shown in Figure 2, where pore size distributions of EC scaffolds obtained at different polymer concentrations are reported.

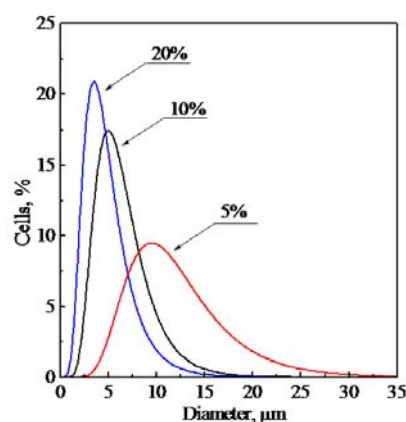


Figure 2: Pore size distribution of EC scaffolds obtained at 200 bar and 35 °C, starting from different polymer concentrations.

Increasing the polymer concentration from 5 to 20 % w/w, the mean pores size varies from 10 to 3 μm and the distributions become sharper.

Once evidenced the effect of polymer concentration, we focused our attention on the effect of process pressure; in particular, we performed experiments at pressures ranging between 100 and 200 bar. From SEM images, it is clear that, for each temperature and polymer concentration tested, increasing the pressure, the mean pores size decreased. An example of these results is reported in Figure 3, where pore size distributions of EC scaffolds obtained at 45 $^{\circ}\text{C}$, 10 % w/w of polymer and at different pressures are shown.

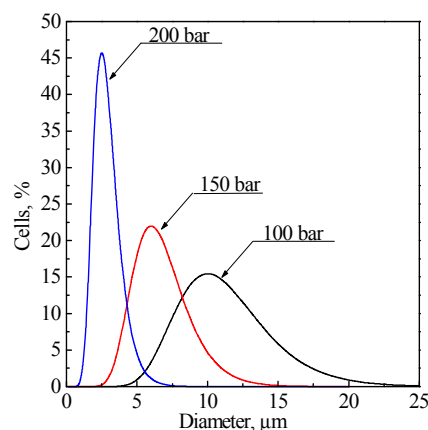


Figure 3: Pore size distributions of EC scaffolds obtained at 45 $^{\circ}\text{C}$, 10 % w/w of polymer and at different pressures.

Increasing the operating pressure from 100 to 200 bar, the mean pores size decreases from 11 to 2 μm . To explain this result, it is necessary to refer to the phase separation theory and to ternary phase diagrams. Indeed, the morphology and the pore size of a phase-separated structure depends on the demixing point inside the miscibility gap of the polymer/solvent/non-solvent ternary diagram. In this case, SC-CO₂ acts as the non-solvent and has the capability of modify the demixing gap with its properties; in particular, when operating pressure increases, the SC-CO₂ solvent power increases too and, as a consequence, the demixing gap in the ternary diagram EC/NMP/SC-CO₂ becomes smaller. A qualitative explanation of these phenomena is reported in Figure 4, where two hypothetical ternary diagrams at different SC-CO₂ pressures are shown.

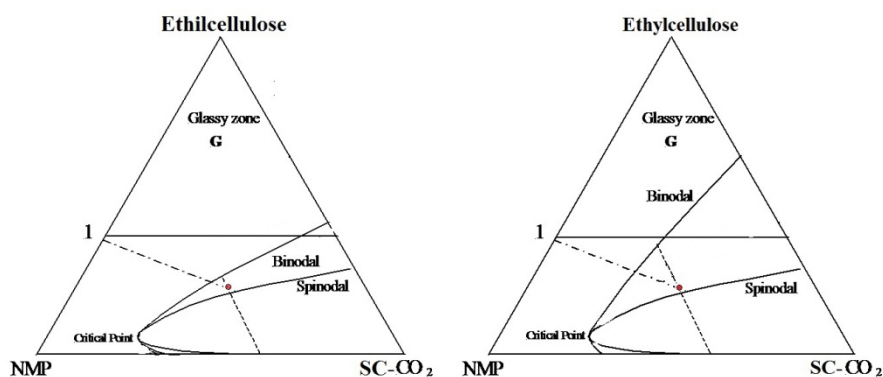


Figure 4: Hypothetic EC/NMP/SC-CO₂ ternary diagrams at different SC-CO₂ pressures: 200 bar (left), and 100 bar (right).

Starting from EC-NMP solution indicated with point 1 in Figure 4, the solution concentration pathway “moves” towards the non-solvent (SC-CO₂) apex. When the SC-CO₂ pressure is higher (200 bar - left diagram of Figure 4), the miscibility gap is smaller (continuous line), and the demixing point (intersection between solution pathway and tie-line) will be located nearest to the polymer-rich part of the binodal line; as a consequence, smaller pores will be generated. On the contrary, when the SC-CO₂ pressure is lower (100 bar - right diagram of Figure 4), the demixing gap is larger and the demixing point will be located farther from the polymer-rich part of the binodal curve, causing the formation of larger pores.

We also analyzed the effect of operating temperature. In particular, we performed experiments at temperatures ranging between 35 and 55 °C. From SEM images, it is evident that, for each pressure and polymer concentration tested, decreasing the temperature, the mean pore size decreased. An example of these results is reported in Figure 5, where pore size distributions of EC scaffolds obtained at 150 bar, 10% w/w of polymer and at different temperatures are shown.

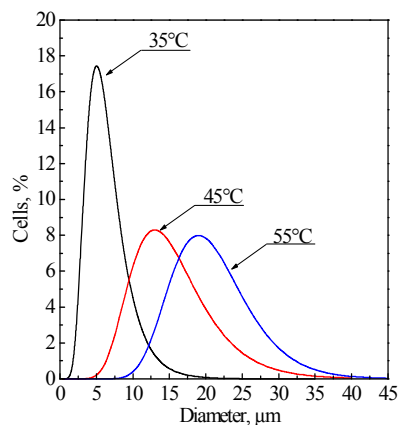


Figure 5: Pore size distributions of EC scaffolds obtained at 150 bar, 10 % w/w of polymer and at different temperatures.

Decreasing the operating temperature from 55 to 35 °C, the mean pores size decreases from 18 to 5 μm. To explain this result, we can make similar considerations to those reported above; indeed, a decrease of process temperature leads to an increase of SC-CO₂ solvent power. As a consequence, a lower temperature means higher solvent power and smaller demixing gap in the ternary diagram EC/NMP/SC-CO₂.

In the last part of the work, we focused our attention on the effect of the organic solvent on the EC scaffolds morphology and mean pores size. Also using chloroform, we verified the feasibility of the process and we obtained EC scaffolds with homogenous cellular structure. We performed experiments at different polymer concentrations, temperatures and pressures, finding results similar to those obtained from EC-NMP solutions. Subsequently, we analyzed the effect of the solvent used, comparing the pore size distributions of EC scaffolds obtained with the two solvents tested. In Figure 6, a comparison between pore size distributions of two scaffolds obtained at the same operating conditions (10 % w/w of polymer, 200 bar and 45 °C) from NMP and chloroform solutions is reported.

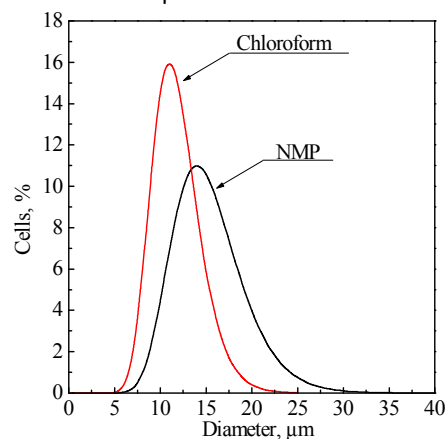


Figure 6: Comparison between pore size distributions of scaffolds obtained at the same operative conditions (10% w/w of polymer, 200 bar and 45°C) from NMP and chloroform solutions.

Using Chloroform, smaller pores are generated; this result was observed for each process parameters combination tested. These phenomena can be explained considering again the phase inversion theory and the ternary phase diagram; indeed, the mutual affinity between chloroform and SC-CO₂ is larger than the mutual affinity between NMP and SC-CO₂. It means that the system EC-Chloroform-SC-CO₂ presents a smaller miscibility gap. As a consequence, once fixed the polymer concentration, pressure and temperature (i.e., fixed the solution pathway inside the ternary diagram), when the miscibility gap is smaller, the demixing

point will be located nearest to the polymer-rich phase, causing the formation of smaller pores (i.e., using chloroform).

4. Conclusions

EC scaffolds were produced using the supercritical CO₂-assisted phase separation method. The results confirmed the feasibility of the process and the advantages with respect to the traditional methods; indeed, scaffolds were generated in short processing times and without residual solvents. Moreover, the capability of modulating scaffolds characteristics was verified.

References

- Caputo G., De Marco I., Reverchon E., 2010, Silica aerogel–metal composites produced by supercritical adsorption, *The Journal of Supercritical Fluids*, 54, 243–249.
- Cardea S., Gugliuzza A., Schiavo Rappo E., Aceto M., Drioli E., Reverchon E., 2006, Generation of PEEK-WC membranes by supercritical fluids, *Desalination*, 200, 58–60.
- Cardea S., Sessa M., Reverchon E., 2011, Processing of co-crystalline and nanoporous-crystalline polymers: Supercritical CO₂ processing of drug loaded membranes based on nanoporous PVDF-HFP aerogels, *Soft Materials*, 9 (2-3), 264-279.
- Cardea S., Baldino L., De Marco I., Pisanti P., Reverchon E., 2013, Supercritical gel drying of polymeric hydrogels for tissue engineering applications, *Chem. Eng. Trans.*, 32, 1123-1128.
- De Marco I., Cardea S., Reverchon E., 2013, Polymer micronization using batch supercritical antisolvent process, *Chemical Engineering Transactions*, 32, 2185-2190.
- Ho H., Ponticello M.S., Leong K.W., 1995, Fabrication of controlled release biodegradable foams by phase separation, *Tissue Eng*, 1, 15–28.
- Hua F.J., Kim G.E., Lee J.D., Son Y., Lee D.S., 2002, Macroporous Poly(L-lactide) Scaffold 1. Preparation of a Macroporous Scaffold by Liquid–Liquid Phase Separation of a PLLA–Dioxane–Water System, *J Biomed. Mater. Res.*, 63, 161–167.
- Kim S.S., Lloyd D.R., 1992, Thermodynamics of polymer/diluent systems for thermally induced phase separation: 3. Liquid-liquid phase separation systems, *Polymer*, 33, 1047–1057.
- Langer R., Vacanti J.P., 1993, Tissue engineering, *Science*, 260, 920-926.
- Ma P.X., 2004, Scaffold for tissue fabrication, *Mater today*, 7, 30-40.
- Mooney D.J., Baldwin D.F., Suh N.P., Vacanti J.P., Langer R., 1996, Novel approach to fabricate porous sponges of PLDA without the use of organic solvents, *Biomaterials*, 17, 1417-1422.
- Pisanti P., Yeatts A.B., Cardea S., Fisher J.P., Reverchon E., 2012, Tubular perfusion system culture of human mesenchymal stem cells on poly-L-lactic acid scaffolds produced using a supercritical carbon dioxide-assisted process, *J. Biomed. Mat. Res. - Part A*, 100A, 2563–2572.
- Prasertmanakit S., Praphairaksit N., Chiangthong W., Muangsin N., 2009, Ethyl Cellulose Microcapsules for Protecting and Controlled Release of Folic Acid, *AAPS PharmSciTech.*, 10(4), 1104-1112.
- Reverchon E., Cardea S., Rapuano C., 2007, Formation of polyvinylalcohol structures by supercritical CO₂ processing, *Journal of Applied Polymer Science*, 104, 3151–3160.
- Reverchon E., Cardea S., 2007, Production of controlled polymeric foams by supercritical CO₂, *The Journal of Supercritical Fluids*, 40, 144-152.
- Reverchon E., Cardea S., Schiavo Rappo E., 2008, Membranes formation of a hydrosoluble biopolymer (PVA) using a supercritical CO₂-expanded liquid, *The J. of Supercr. Fluids*, 45, 356-364.
- Reverchon E., Cardea S., 2012, Supercritical fluids in 3-D tissue engineering, *The J. of Supercr. Fluids*, 69, 97-107.
- Schugens C., Maquet V., Grandfils C., Jerome R., Teyssie P., 1996a, Polylactide macroporous biodegradable implants for cell transplantation. 1. Preparation of macroporous polylactide supports by solid–liquid phase separation, *Polymer*, 37, 1027–1038.
- Schugens C., Maquet V., Grandfils C., Jerome R., Teyssie P., 1996b, Polylactide macroporous biodegradable implants for cell transplantation. II. Preparation of polylactide foams by liquid–liquid phase separation, *J. Biomed. Mater. Res.*, 30, 449–461.
- Zeng J., Xu X., Chen X., Liang Q., Bian X., Yang L., Jing X., 2003, Biodegradable electrospun fibers for drug delivery, *J. Control. Release*, 92, 227-231.